JOURNAL OF MATERIALS SCIENCE 27 (1992) 6735–6742

Tribology of amorphous diamond films grown or modified by ion implantation

J. C. PIVIN
CSNSM, IN2P3/CNRS, Batiment 108, 91405 Orsay Campus, France

The friction and wear resistances of amorphous diamond films grown by quenching of an intense laser-plasma or by ion implantation were correlated to their thickness and structure. Their adherence to a $Ti_{0.85}Al_{0.11}V_{0.04}$ alloy is assisted by an interfacial layer of TiC precipitates. This adherence can be improved by a further irradiation promoting the growth of the Ti–TiC composite layer by radiation-enhanced diffusion in the metallic matrix. Nitrogen implantation in the substrate has an additional catalytic effect on the carbide nucleation. However, damaging the carbon film itself or doping it with nitrogen do not improve the mechanical properties and are rather detrimental for electronic properties.

1. Introduction

Many papers already account for the high abrasion resistance and the low friction coefficient of hard plastics known as diamond-like carbon coatings (DLCs, which would be more properly named DLHC as they are hydrocarbons) [1, 2]. They are generally less rough than polycrystalline diamond films and more continuous. However, true DLCs, containing no hydrogen, exhibit additional advantages. Because they are obtained essentially by ionic bombardment of substrates under carefully selected conditions (described below), the removal of contamination films and the intermixing with substrate layers at the beginning of the process provide them with a better adherence than that of coatings being simply deposited. Such a quality is especially required for any other mechanical application than cutting tools. One application of high interest, when considering the cost of ion-beam treatments, is the protection of bone prostheses. The coating must not abrade the counterpart and constitute a continuous barrier against the reaction of blood with the substrate (generally made of titanium alloys) and its clotting and subsequent consequences. Any DLHC would also be a good candidate if sufficiently adherent. Other biomedical pieces made of the same alloys or of steels which could be coated are heart valves and surgical instruments.

It is not the purpose of the present paper to investigate the resistance of true DLC grown by implantation of an ion beam (IB) or of ions issued from an intense laser-plasma (LP), in biological environments. In these preliminary tests, the resistances to friction and wear of these films have been simply compared in dry air as a function of three parameters: (i) their amorphous graphite (a-G) content (a hypothetical entity which would consist only of sp2-bonded atoms, in comparison with amorphous diamond, a-D, containing only sp3-bonded atoms); (ii) their thickness; (iii) the improvement of surface roughness and adherence provided by additional irradiation. LP films are the most diamond-like [3–7] but transmission electron micrographs or scanning tunnelling micrographs show that their surfaces exhibit more protrusions than IB films [8]. The present tests demonstrated that the friction coefficient of LP films is subsequently higher and they are less resistant to spallation (even when thicker) than IB films.

On the other hand, improvements of friction and wear properties have been reported for DLHC films grown by vapour deposition techniques after irradiating them with nitrogen ions at energies in the 100 keV range [9]. The effect was attributed to an increase in the amount of sp3-bonded atoms in the film when doped with nitrogen, and to damage (especially when irradiation was performed at low temperatures). However, our own investigations of the optical and transport properties of irradiated films indicate the opposite trend. We suspect that the main effect is the building of interfacial layers with a mixed nature:

(i) soft a-G formed at the expense of a-D in a regime of linear collision cascades. Indeed the proper regime for simulating the thermodynamical conditions of diamond growth is more probably a displacement spike, i.e. a dense cascade where all atoms are moving. Such spikes occur, for instance, when implanting C^+, or C^{n+} in LP experiments, at energies slightly over 1 keV (the content of a-D in both types of implantation film attaining 85% in these optimal conditions, they are often called a-D films to distinguish them from other "DLC");

(ii) carbides formed by ballistic plus radiation-enhanced diffusion of substrate atoms, when the damages are created beyond the interface. The destabilization of a-D near the interface can help the growth of this carbide. Readers who are not accustomed to the notions of linear cascades, spikes and of ion-induced diffusion should refer for further information to Kelly [10], and Pivin and Riviere [11].

0022–2461

2. Specimen preparation and analysis

The substrates of all films were sheets of a $Ti_{0.85}Al_{0.11}V_{0.04}$ alloy, polished mechanically with SiC papers, then electrolytically in a Blackburn bath (60% methanol + 35% *n*-butyl alcohol + 5% perchloric acid at − 40 °C under a voltage of 15 V). The riders were cylinders ended by a hemispherical cap with a radius of curvature of 1 cm, machined from the same alloy and polished using the same procedure. All these riders were coated with 1 μm thick LP films. Riders without coating used in preliminary tests wore too quickly under the friction conditions described below. Tests under the same load, F, and at the same speed with SiC balls exhibiting a radius of curvature, R, of 4 mm were too severe: the Hertzian contact pressure varies as $F^{1/3}R^{-2/3}$.

An apparatus built at the University of Texas at Dallas [5, 6] was used for LP implantations. The beam of a Q-switched Nd–YAG laser is focused on a graphite target in an ultra-high vacuum, and its intensity must be kept above 10^{11} W cm^{-2} to obtain a plasma composed essentially of C^{3+}, C^{4+} ions with a kinetic energy around 1 keV. Higher ionization and heating of the plasma is ensured by a discharge through its path. Films deposited at lower intensities or by exposing substrates to the peripheral part of the plasma are similar to glassy carbon (about 15% a-D + 85% a-G). By using a diaphragm and a rotating holder, substrates can be illuminated by only the hotter core of the plasma. Under such conditions, a-D is deposited homogeneously at a rate of 0.5 μm h^{-1} over areas of 100 cm^2.

IB implantations of C^+ ions filtered in mass and energy (with respective resolutions of 1 a.m.u. and 10 eV) were performed under a vacuum of 10^{-7} torr (1 torr = 133.322 Pa) in one of the machines built at Orsay. These implantors provide beams of relatively high intensities, which is typically 50 μA in the case of C^+ ions. The focused beam of 1 mm is electronically scanned over areas of a few square centimetres, giving deposition rates 100 times lower than by LP implantation. Thus films thicker than 1 μm are prepared only for special experiments, and the thickness was kept between 0.35 and 0.25 μm for all tests presented here. The implanted fluence was the same for all energies of IB implantation but the part removed by self sputtering increased with this parameter (Table I).

Some LP films with thicknesses restricted to 0.1–0.2 μm were irradiated with N^+, C^+ or Ne^+ ions under three different conditions:

(i) a single irradiation with 2×10^{16} ions N^+ cm^{-2} at an energy of 100 keV. TRIM simulations of the ions slowing down [12] for a bilayer of 0.10 μm carbon over titanium corresponding to this irradiation, allowed us to estimate that defects were produced essentially in the metallic substrate at a mean depth of 50 nm beyond the interface. The maximum concentration of nitrogen at a mean implantation depth of 180 nm was 3.3% for this fluence;

(ii) a similar irradiation with 5×10^{16} ions C^+ cm^{-2} at 150 keV. In this case defects were created at a mean depth of 100 nm beyond the interface because the film was 0.15 μm thick, the mean range of ions, R_p, was 290 nm and their concentration at R_p was 6%;

(iii) a double irradiation with 2×10^{16} ions N^+ or Ne^+ cm^{-2} at 150 keV and 10^{16} ions of the same element at 75 keV. Ranges of damage, R_d, and of ions, R_p, through carbon layers 0.15 μm thick were, respectively, for Ne: $R_d = 190$ nm, $R_p = 220$ nm at 150 keV, and $R_d = 90$ nm, $R_p = 130$ nm at 75 keV; for N: $R_d = 220$ nm, $R_p = 250$ nm at 150 keV, and $R_d = 100$ nm, $R_p = 145$ nm at 75 keV. These ranges are very similar, but Ne^+ ions implanted at 75 keV created only defects in the carbon film, while N^+ ions implanted at the same energy could have modified the chemical bonding.

The areal densities of carbon atoms were measured by Rutherford backscattering (RBS) and nuclear reaction analysis (NRA), as were the amount of contaminants, in all types of film. In not any case the hydrogen concentration, measured using the $^{15}N(p, \alpha, \gamma)^{12}C$ reaction, exceeded 5H/1000 C. The areal density of oxygen and nitrogen, measured by d.p. reactions were also lower than on bare substrates: 5×10^{15} atoms cm^{-2} and most part was segregated at the interface.

Rutherford backscattering spectra provided additional information on the interdiffusion of carbon and substrate atoms at the interface, especially when col-

TABLE I

Nature of film	Ions	Implantation or irradiation fluence (10^{16} cm^{-2})	Energy (keV)	Film thickness (μm)	Friction properties	
					Coefficient	Life time (cycles)
Implantation	C	500	0.10	0.36	0.12 ± 0.04	40 ± 20
	C	500	0.50	0.28	0.20 ± 0.10	1400 ± 400
	C	500	1.00	0.26	0.20 ± 0.10	4500 ± 1000
	C	500	2.00	0.24	0.30 ± 0.05	6000 ± 2000
Laser-plasma	none			0.10		
	none			0.15	about 0.15	1 to 10
	none			0.42	0.40 ± 0.05	1800 ± 500
	none		0.65		0.60 ± 0.10	6000 ± 2000
	N	2	100	0.10	0.10 ± 0.02	500 ± 100
	N	2 + 1	150 + 75	0.15	0.20 ± 0.05	50 ± 20
	Ne	2 + 1	150 + 75	0.15	0.20 ± 0.05	2500 ± 800
	C	5	150	0.15	about 0.12	1 to 10

lecting the scattered He^+ ions at a grazing angle of 97° with respect to the incidence direction (normal to the surface). The path travelled by ions after the scattering event at a given depth, x, is higher than for ions collected at angles of 170°–160° (more conventional conditions), and connectively the energy loss to electrons during their exit. Consequently, the depth-resolution is better with a grazing collection, but the probed range of depths for a given incidence energy decreases. This parameter was chosen according to the film thickness in our experiments. Note that when it exceeds 3 MeV (for investigating carbon films thicker than 0.4 μm with a grazing collection), the scattering cross-section of carbon atoms no longer obeys the Rutherford law, such that one can only use conventional simulation programs [21] for fitting that part of the spectra relative to substrate atoms. When the overlapping spectra of He^+ ions scattered by the substrate and carbon atoms can be fitted simultaneously, it helps to confirm the detected gradients. Examples of $Ti_{0.85}Al_{0.11}V_{0.04}$ coated by LP and IB implantation are shown in Figs 1 and 2.

An interdiffusion is observed at the interface, as also for Si, ZnS, or other types of substrate. This cannot be ascribed to a simple ballistic mixing which would concern ranges of, at most, 5 nm (4×10^{16} atoms cm^{-2} in terms of densities) or to the surface roughness. Topography recordings on lengths equal to the diameter of the He^+ beam allowed estimation of its average value, R_a, to be 20–40 nm depending on the substrate. However, R_a includes low-frequency oscillations (due to the initial polishing) which are the same for the coating surface and the interface. Both remain parallel, because the mean height of the film asperities,

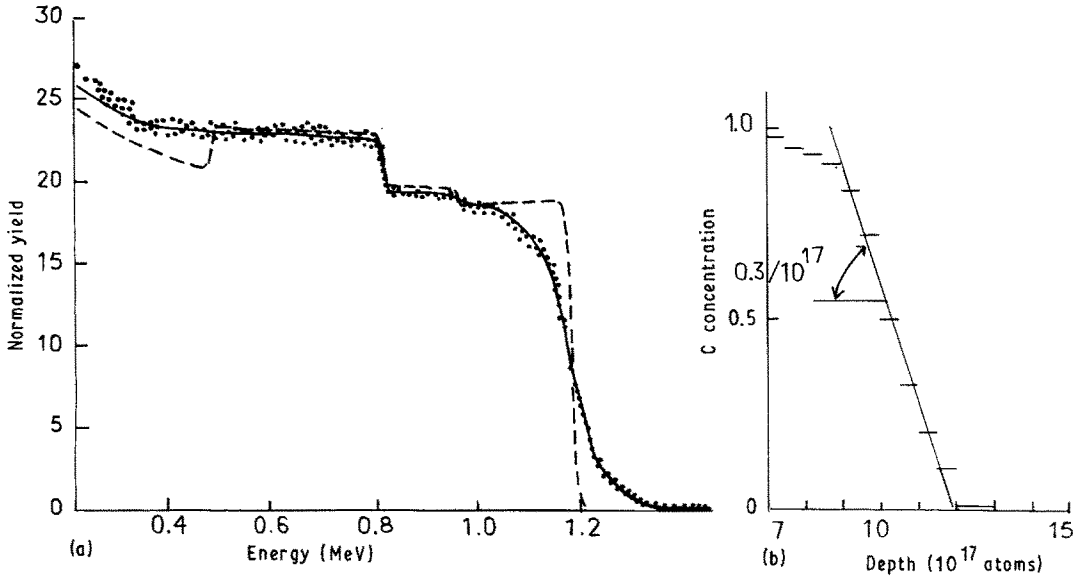

Figure 1 (a) Rutherford backscattering spectrum on a film built by LP quenching (. . .) The energy of the He^+ incident ions was 1.8 MeV, backscattered ions were collected at an angle of 97°. The film thickness measured by means of a stylus technique was 0.19 μm. (——) The fit to the experimental curve which was obtained with the concentration profile shown in (b). (– – –) The same total number of carbon atoms cm^{-2} if there was no mixing.

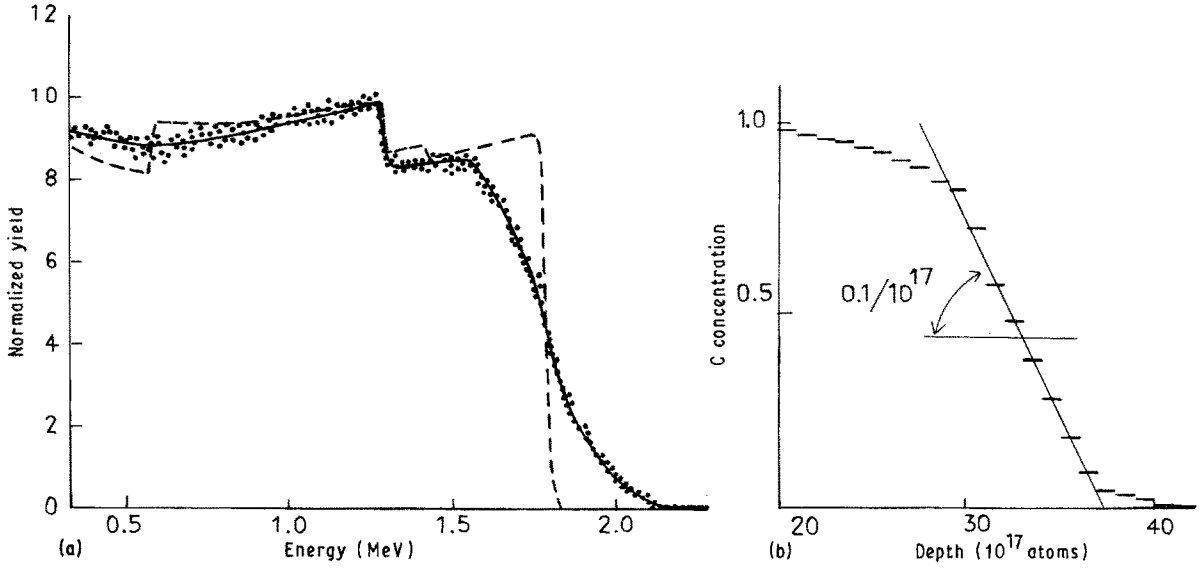

Figure 2 (a, b) Rutherford backscattering spectrum on a film built by IB implantation of 5×10^{18} C^+ ions cm^{-2} at an energy of 1 keV. For key, see Fig. 1, but the energy of analysing ions was 2.8 MeV because the film was thicker. The mean slope at mid-height of the gradient, used as a comparison parameter, is twice as small as for the LP film of Fig. 1.

measured by scanning tunnelling microscopy (STM) [8], is around 10 nm. It is of the same order of magnitude as the size of nodules constituting these a-D films: 50 nm for all LP films and 25 nm for IB implantations at 1 or 2 keV, as shown by TEM on replicas (Fig. 3). These nodules are due only to an heterogeneous growth process around nuclei, because no change in chemical binding could be detected at their periphery by electron energy loss spectroscopy (EELS) with a high spatial resolution (in TEM on thin foils). Their size is determined by the statistical distance between initial nuclei. Note also that a consequence of this growth mechanism is a mismatch in the piling of atoms at their boundary, accounting for the density defect of a-D films with respect to diamond (1–1.3 instead of 2×10^{23} atoms cm^{-3}). However, there are only a few particles of a-G in these films.

The interfacial gradient measured by RBS is nearly an error function, but its mathematical analysis for calculating a diffusion coefficient in a homogeneous solid solution would be illusory. Indeed TEM observations (on foils prepared by electrolytic dissolution of substrates in a Blackburn bath in the case of Ti or TiAlV) allowed to evidence precipitations at interfaces with Ti, TiAlV or Si. The carbide particles, with a mean size of 20 nm, are scattered along the interface, but they are likened to a continuous layer with a mean composition at the square millimetre scale of RBS analysis. Their nature will be discussed later after concluding remarks concerning the width of interfacial layers for the various types of films. The mean slope at half height of the RBS concentration gradients was generally two times steeper for LP films than for IB ones, whatever the substrate (Si, ZnS, Ti or TiAlV). RBS analysis of the same LP coatings on various substrates after ion irradiation, showed that the sputtering of superficial layers was not significant for ions of 100 or 150 keV and of only 0.02 μm (2×10^{17}C atoms cm^{-2}) for irradiation with 10^{16} ions of 75 keV. The mixing of interfacial layers was also much less than during the deposition of carbon. The apparent width of the interfaces remained generally constant or decreased slightly in some cases. This result is attributed to smoothing of surface asperities, but topography changes could not be detected on replicas.

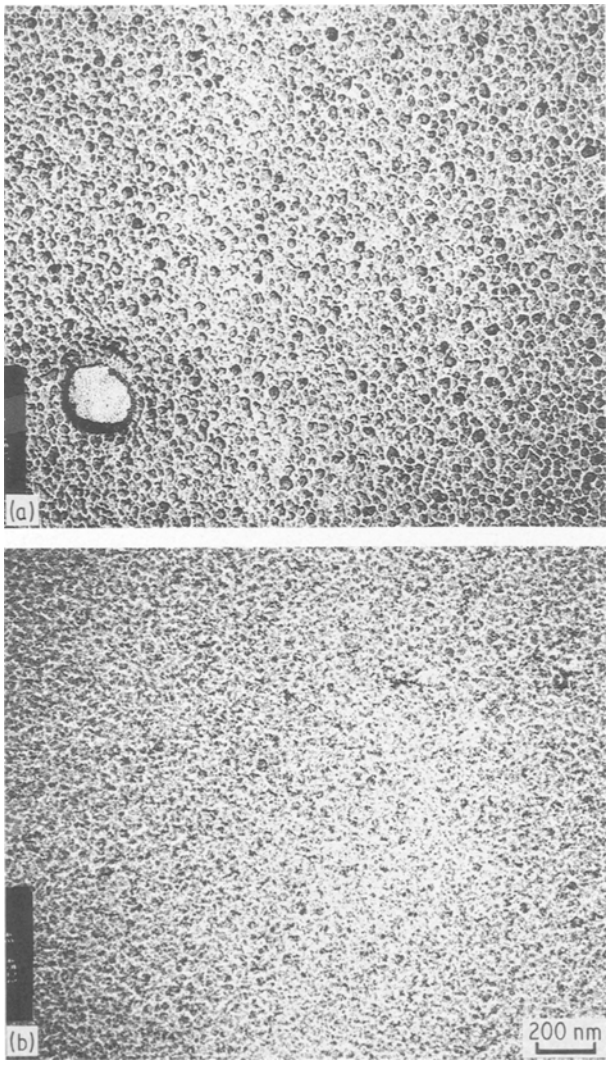

Figure 3 Transmission electron micrographs of imprints (taken on a plastic tape, which was coated with evaporated carbon and silver, then dissolved in acetone) showing the surface topography of the same films as in Figs 1 and 2: (a) LP film, (b) IB film.

The crystallographic nature of interfacial precipitations and their epitaxy relationships with matrixes of pure titanium or TiAlV were assessed by recording several diffractograms at different tilt angles of the observed foils. In all cases a face-centred cubic phase of the TiN or TiC type was identified, and the relationships were the most simple ones between the directions of close packing. (1 1 1) planes of the precipitates were parallel to (0 0 0 1) or (1 0 $\bar{1}$ 0) in the α–Ti matrix. Fig. 4 shows diffraction patterns of both phases and a dark-field image of the particles obtained by selecting their (1 1 1) diffracted beam for an LP film irradiated with N^+ ions at 100 keV. This example was chosen because the areal density of precipitates was highly enhanced after this particular irradiation, while they were more scarcely distributed in unirradiated specimens or after Ne^+ irradiation. Diffraction patterns were conclusive, but good pictures of the precipitates with their own diffracted beams could not be obtained. In the particular case of the specimen irradiated with N^+ ions, a finely subdivided composite layer was built up over a thickness near 100 nm (all parts of the foil being transparent to electrons) compared to less than 20 nm for other specimens. However, EELS analysis on precipitates shown in Fig. 4 indicated that they contained an higher concentration of carbon than nitrogen. An artefact due to the contribution of the carbon film to the recorded spectrum cannot be invoked, because the carbon absorption edge exhibited oscillations characteristic of a crystalline phase, contrary to spectra recorded on the film itself.

Moreover, nitrogen implantation at similar concentrations in uncoated specimens did not lead to a nitride precipitation [13]. Nitrogen remains in solid solution up to a concentration of 15% N, then precipitates of the quadratic phase, Ti_2N, are formed, and the cubic nitride, TiN, appears only above 30% N. A straightforward conclusion is that TiC precipitates are formed by radiation-enhanced diffusion after N^+ irradiation. In addition to the creation of point defects

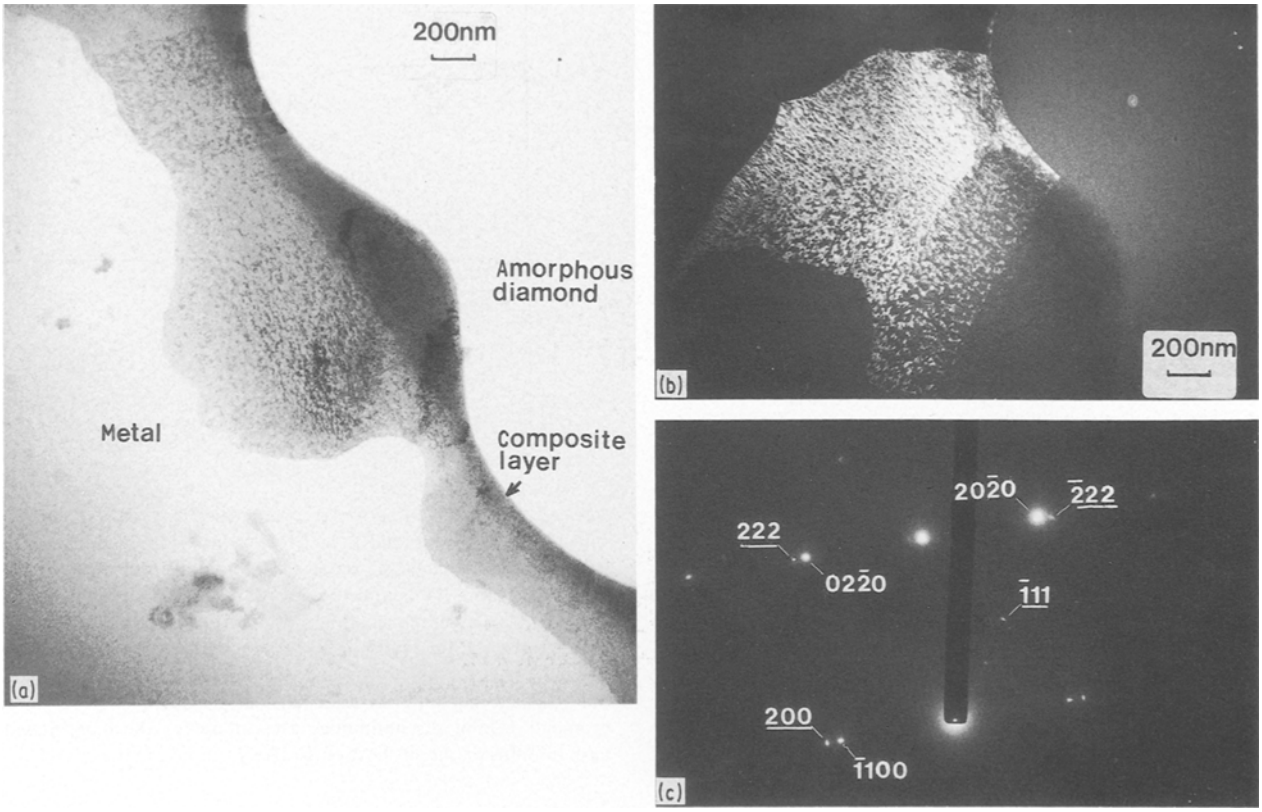

Figure 4 Transmission electron micrographs: (a) bright field, (b) dark field, and (c) diffraction pattern of the same area as in (b), of precipitates formed near the interface in a TiAlV substrate coated with 0.1 μm carbon by LP then irradiated with 10^{16} N^+cm^{-2} of 100 keV. The indices of planes relative to the [0 0 1] section of the cubic precipitates are underlined on the pattern. (a) shows that a continuous composite layer is built at the interface.

and dislocations, which are also observed in foils of specimens irradiated with Ne^+, nitrogen plays a catalytic role in the nucleation of the carbide. It probably segregates on dislocations. Another interesting feature of specimens irradiated with N^+ at 100 keV was their higher mechanical resistance after electrolytic thinning. Transparent areas remained complete over 1 mm in width, while the carbon film was quite systematically rolled or broken under the effect of internal stresses on other specimens.

3. Friction and wear

We have conceived a tribometer with the following specifications: (i) a high stiffness of the assembly allowing application of loads between 1 and 100 N ($\pm$ 0.2 N) on motionless pins with various shapes (by using interchangeable holders). The applied pressures (if assumed elastic) are much higher than in any test performed on hard coatings: 2–10 GPa for $R = 1$ cm, 10–50 GPa for $R = 1$ mm, calculated with the elastic modulus and Poisson's ratio of $Ti_{0.85}Al_{0.11}V_{0.04}$. These values always exceed the yield stress of any metallic substrates and of most ceramics;

(ii) a motion mode of the test specimens allowing homogeneous rubbing of an area of several square millimetres and measurement of friction or wear resistances which are statistically significant. For this purpose, the sample holder is moved by step-to-step motors along two directions X, Y, in a plane perpendicular to the direction of load application. The type of motion is chosen at will and repeated under the control of a programmable interface. For instance, each cycle of the program is constituted by a travel of 3 mm along X followed by 50 μm along Y, then $-$ 3 mm along X followed by 50 μm along Y, which is repeated 30 times to scan an area of 3 mm × 3 mm. Successive paths of the rider along Y necessarily overlap because the area of contact is always over 100 μm. Thus asperities initially present and formed during each path along X (crushed particles, pile-up of plastic deformation) are compressed during succeeding motions along $-X$. Moreover, the automatic repetition of the cycle ensures the homogeneity of the loading conditions at the micrometre scale over the whole area of the scan.

The friction coefficient is recorded continuously along the X direction, while any friction resistance along Y is suppressed via an appropriate setting of the rider and gauge holders. The amount of wear after incremented numbers of scans can be assessed by RBS analysis of wear tracks or tactile profilometry.

The two methods have been used in present tests but did not provide interesting results until now. Whatever the type of carbon film, a few hundred nanometres were abraded during the first 100 cycles (under a load of 1 N and with the type of cycle given above as an example). Then the wear kinetics decreased to zero and the surface roughness remained unchanged until a critical number of cycles, when the films were thicker than 0.2 μm. This number being, in some cases, several thousands, and the final crushing

of the film taking place within 100 cycles, the variation of friction coefficient appeared a more direct method for measuring the lifetime of each film.

However, RBS and SIMS analysis on wear tracks gave more information on the wear process. In the case of thick a-D films (0.2–1 μm) deposited by LP or by IB implantations at energies over 500 eV, the depth profile of the composition remained unchanged until the cycle number threshold. But films resulting from implantations at lower energies contain a higher concentration of a-G (as shown by several techniques used for probing their dielectric properties) (3, 4, 7, 14). One can reasonably suppose that they are softer than the former, so that they are less resistant to wear (Table I). They probably cracked locally since the beginning of tests. Indeed a gradient of oxygen diffusion in the underlying $Ti_{0.85}Al_{0.11}V_{0.04}$ substrate was detected before 20% of the carbon film was worn (after 100 cycles for a 500 eV implantation film). Its extent increased with the duration of the test until removal of the film. Such a behaviour has already been observed for other types of ceramic coating on this alloy: TiN, TiC, TiB formed by IB implantation or by chemical vapour deposition [13, 15]. Local cracks in a hard coating are formed every time that two requirements are answered simultaneously [16]: (a) the extension of the field of plastic deformation beyond the interface, and (b) a subcritical ratio of substrate/film hardness. Note already that both factors are not independent because the former also depends on the film thickness. Hard films inhibit wear of their substrate as long as they are not abraded, if they have a minimal thickness. This minimal value decreases with the ratio defined in (b).

This criterion has, in fact, been defined for plastic films. If they are so stiff that even the deformation of the substrate remains nearly elastic, they do not crack during unloading (at the end of the contact in each point of the track). They can only be worn by two processes: (c) the abrasion of asperities submitted to high concentrations of stress, and (d) the delamination of interfacial layers by fatigue under quasi-elastic conditions of loading. Both processes are probably involved in the case of the hardest films studied here. A significant oxidation of the substrate was recorded by SIMS only at the beginning of tests where more than 90% of the film was already worn or when its initial thickness was less than 0.2 μm (Fig. 5).

Typical variations of the friction coefficient, μ, recorded on relatively thick films (over 0.2 μm) are shown in Fig. 6. It was generally two times lower at the beginning of tests for all IB films than for LP ones. The most probable reason is their lower roughness (as seen by STM, TEM), but also their higher plasticity. However, the coefficient of the hardest IB film increased sometimes up to the value characteristic of LP ones. For both types of film, a steep decrease in this coefficient was thereafter recorded, at the moment where they began to spall locally. Then it exhibited fluctuations across the rubbed area, and finally became more stable when reaching the characteristic value of bare substrates in contact with a-D riders: 0.5 ± 0.1.

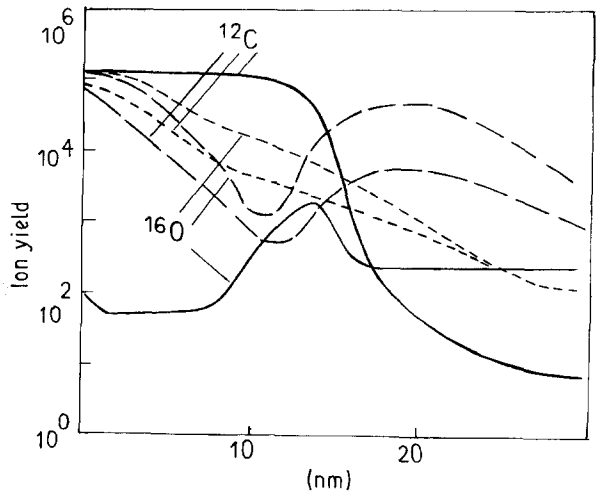

Figure 5 Variations of secondary ion emissions versus sputtering time by Ar^+ ions, recorded on an LP film with an initial thickness of 0.15 μm: (——) out of the track, (– – –) two different areas of the track just before the complete removal of the carbon film. Before friction, there is only a small bump in the oxygen (and hydrogen) concentration at the interface, corresponding to a thin oxide layer, but huge gradients of oxygen and carbon diffusion in the substrate are observed thereafter. In some parts of the track (— — —) these gradients exhibit discontinuities accounting for the oxygen and carbon diffusion along short paths like grain boundaries.

These friction curves can be considered as school cases illustrating rheological models developed a few years ago [16–20]. Let us explain in more detail the concepts evoked in points (a) and (b). The depth of plastification in a plane material submitted to a static or tangential indentation by an asperity (supposed undeformable) depends critically on the angle, θ, made by the asperity surface and the loading direction. Moreover, the plastic surface shrinks at the centre of the contact, but piles up at the periphery. The height, h, of this pile-up and its angle, φ, with respect to the initial surface, increase when a tangential motion is imposed to the asperity. The coefficient, μ, increases with φ until a critical ϕ_c value for which the pile-up is cut by the asperity. The sharper the asperity (i.e. the smaller θ), the lower is the critical ϕ_c for a given load or, respectively, the steeper is the increase of φ toward ϕ_c when increasing the load. Now, when the plastic material is covered by a hard coating, μ varies with the ratio of h to the coating thickness, t, as with the cycle number in Fig. 5. For low values of h/t, the coefficient μ and angles φ, ϕ_c are intrinsic to the hard material; generally μ is high. When increasing h/t (via an increasing load or decreasing θ, t) one can observe a decrease of μ because the more plastic substrate accomodates the deformation. But connectively φ increases, and for a critical value $(h/t)_c$ near 4, whatever the ratio of hardness, the coating is perforated. Theoretically, μ exhibits an abrupt decrease for subcritical h/t if accounting only for a resistance to ploughing and cutting, while the wear kinetics increases. But μ can also increase if there is a component of adhesion to the friction resistance, as in contacts between an indentor (the rider) coated with a-D and a bare titanium surface.

These variations of μ as a function of t for hard coatings are well known by tribologists. They are also

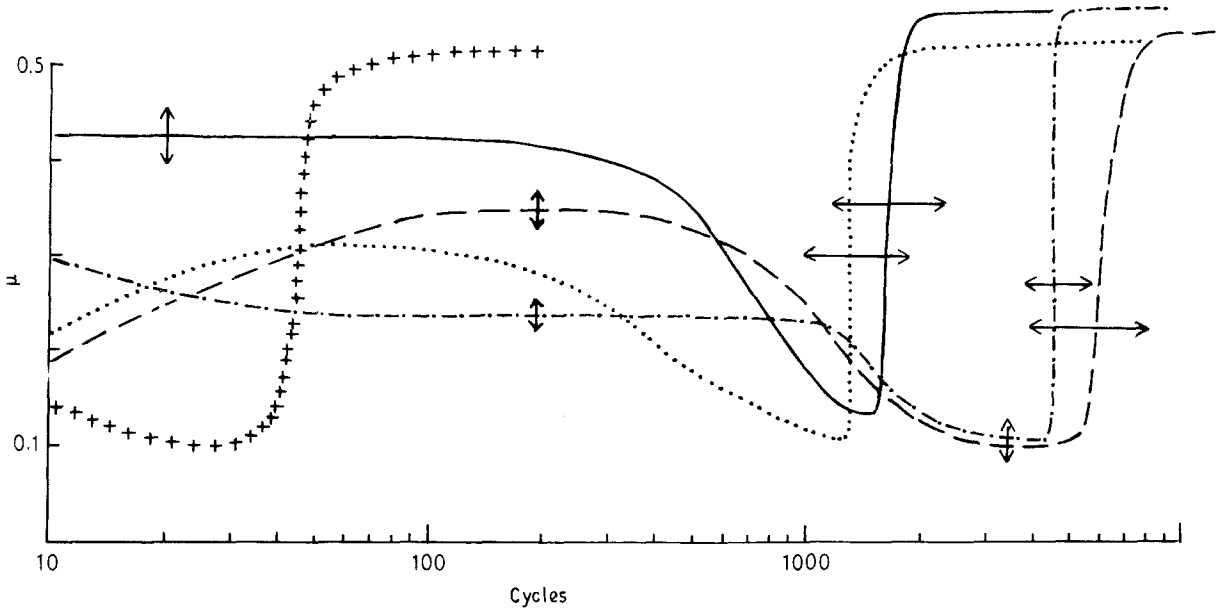

Figure 6 Variations of friction coefficients recorded on films with a thickness of 0.25–0.35 μm formed by IB implantation at (+) 100 eV, (·) 500 eV, (—·—) 1000 eV, (— — —) 2000 eV and (——) an LP film with a thickness of 0.4 μm. Vertical error bars correspond to fluctuations of the friction coefficient along the track, and horizontal ones to variations in the lifetime of these films. Variations of μ from one test to another are not shown on the figure but are summarized in Table 1: they are dependent on the conditions of LP deposition on riders.

verified in the present study when comparing LP films with various initial thicknesses (Table I). For $t = 0.1$ μm, h/t is in the optimal range between h/t intrinsic to the carbon film and $(h/t)_c$: $\mu = 0.10 \pm 0.02$. When $t = 0.2$ μm, μ takes a value intrinsic of contacts between a-D surfaces: 0.40 ± 0.05. But continuous variations of μ on a same film, accounting for this concept, have never been recorded before to our knowledge. Generally, other parameters hamper the verification of theoretical models, among which the formation of wear debris, and the increasing roughness of the track. In the present investigation, debris were systematically removed from the track because of the scanning motion and of their low adherence to the rider (as shown by SEM). SEM images and topography recordings by means of a stylus technique also showed that the tracks remained smooth until the coating was perforated. We conclude this discussion of the variation of friction properties of a-D films with their thickness, by stating that they are interesting in two respects. First, their wear resistance is ten times higher than that of TiN or TiC coatings when comparing them under identical conditions (including thickness and substrate). Even if the friction coefficient of LP films is high, they are good candidates for many applications. Second, they are proper for testing rheological models.

If considering the effects of ion irradiation on friction properties, they are in perfect agreement with ideas developed in Section 1 and with the observed modifications of dielectric properties. The effects can be summarized as follows.

1. There is no beneficial effect of doping the film with nitrogen when it already contains a high percentage of sp3-bonded atoms (about 85% in LP films).

2. Under similar irradiation conditions, a greater improvement is obtained with Ne^+ ions than with N^+. They have the same effect on the superficial roughness, but Ne^+ ions are slightly more efficient at displacing atoms at the interface (R_d is shorter).

3. Under optimal conditions for creating defects at the interface (at an energy of 100 keV through a 0.10 μm thick film), the lifetime of films increases by more than a factor 500. Less severe conditions of friction would have to be used for refining the value of this improvement and the useful irradiation fluence. When damage is formed at too great a depth, as in the case of a 0.15 μm thick film irradiated with 150 keV C^+ ions, it is no longer efficient for inducing the diffusion of titanium towards the interface.

4. Conclusion

The friction coefficient of a-D films depends critically on their thickness and surface roughness. The observed variations of μ as a function of the initial thickness, and as they are progressively abraded, obeys models of rheology more perfectly than for any other type of coating.

As foreseen, collision cascades only have a beneficial effect on the adhesion of films when they occur essentially in the substrate near the interface. Similarly, it is more useful to dope the metallic underlayers with nitrogen than the film itself. It seems to play a catalytic role in the nucleation of carbide particles. The thickness of the composite Ti–TiC layer increases, and also, therefore, its efficiency as a mechanical buffer.

Additional improvements due to a higher amount of residual defects when irradiation is performed at low temperatures must be considered in further investigations, and also those due to irradiation at very low energies. The latter would induce displacement spikes at the extreme surface, removing asperities of LP films and destroying their nodular structure. Any structural defect constitutes a nucleus for cracks. If the diamond-like population at the surface decreases slightly, the

friction coefficient would also decrease. Indeed, the tested material would become constituted of three layers: a soft and lubricating one of a-G (with a coefficient of 0.1, like films formed by implantations at 100–500 eV), over a hard layer of a-D, protecting against wear both the lubricant film and the underlying substrate.

Acknowledgements

We thank Ping Zhen and Marie Christine Sainte-Catherine, for their kind help in TEM experiments, G. Rautureau in SIMS analysis, and Odile Kaitazoff, Dominique Ledu, Marylu Allouard, Tae Jong Lee, Farzin Davanloo and Carl Collins for the carbon depositions.

References

1. "Proceedings DIAMOND 90 and 91 Conferences", *Surface Coating Technol.* **47** (1991) and *Diamond and Related Materials* 1–2 (1992).
2. "NATO Advanced Institute on Diamond and Diamond-like Films and Coatings", NATO-ASI Series B: Physics 266 (Plenum Press, New York, 1991).
3. J. C. PIVIN, M. SPIRKEL, M. ALLOUARD and G. RAUTUREAU, *Appl. Phys. Lett.* **57** (1991) 2657.
4. J. C. PIVIN, J. L. STEHLE, J. P. PIEL and M. ALLOUARD, *Phil. Mag. B* **64** (1991) 1.
5. F. DAVANLOO, E. M. JUENGERMAN, D. R. JANDER, T. J. LEE and C. B. COLLINS, *J. Appl. Phys.* **67** (1990) 2081.
6. *Idem, J. Mater. Res.* **5** (1990) 2398. See also [1].
7. J. C. PIVIN, M. ALLOUARD and G. RAUTUREAU, *Surface Coating Technol.* **47** (1991) 433.
8. C. B. COLLINS, F. DAVANLOO, D. R. JANDER, T. J. LEE, J. H. YOU, H. PARK, J. C. PIVIN, K. GLEBOL and A. P. THOLEN, *J. Appl. Phys.* 1992, in press.
9. M. IWAKI, K. TAKAHASHI and A. SEKIGUCHI, *J. Mater. Res.* **5** (1990) 2562.
10. R. KELLY and M. FERNANDO DA SILVA (eds), "NATO Advanced Institute on Materials Modification by High-Fluence Ion Beams", NATO-ASI Series E: Applied Sciences 155 (Kluwer Academic Dordrecht, Boston, London, 1989).
11. J. C. PIVIN and J. P. RIVIERE, in "Congrès de la Societé Français de Physique", *Editions de Phys.* **199** (1986) p. 199.
12. J. F. ZIEGLER, J. P. BIERSACK and Y. LITTMARK, in "The Stopping and Range of Ions in Solids 1", edited by J. F. Ziegler (Pergamon Press, New York, 1985).
13. J. C. PIVIN, *J. Mater. Sci.* **25** (1990) 2743.
14. J. C. PIVIN, T. J. LEE and R. E: Applied Sciences 155 (Kluwer Academic Dordrecht, Boston, London, 1989).
11. J. C. PIVIN and J. P. RIVIERE, in "Congrès de la Societé Français de Physique", *Editions de Phys.* **199** (1986) p. 199.
12. J. F. ZIEGLER, J. P. BIERSACK and Y. LITTMARK, in "The Stopping and Range of Ions in Solids 1", edited by J. F. Ziegler (Pergamon Press, New York, 1985).
13. J. C. PIVIN, *J. Mater. Sci.* **25** (1990) 2743.
14. J. C. PIVIN, T. J. LEE and R. CANET, *Europhys. Lett.* **17** (1992) 359.
15. F. PONS, J. C. PIVIN and G. FARGES, *J. Mater. Res.* **2** (1987) 580.
16. J. C. PIVIN, in "NATO Advanced Institute of Materials Modification by High-Fluence Ion Beams", edited by R. Kelly and R. Fernando da Silva (Kluwer Academic, Dordrecht, Boston, London, 1989) p. 509.
17. D. LEBOUVIER, thesis, Nice (1987).
18. M. DE VATHAIRE, F. DELAMARE and E. FELDER, *Wear* **66** (1981) 55.
19. J. M. CHALLEN and P. L. B. OXLEY, *ibid.* **53** (1979) 229.
20. B. AVITZUR, C. K. HUANG and Y. D. ZHU, *ibid.* **95** (1984) 77.
21. L. R. DOOLITTLE, *Nucl. Instrum. Meth.* **B45** (1990) 1.

Received 15 October 1991
and accepted 18 March 1992